COMISSIONING OF THE PHOTO-CATHODE RF GUN AT APS*

Y. Sun#, J. Dooling, R. Lindberg, A. Nassiri, S. Pasky, H. Shang, T. Smith, A. Zholents
Advanced Photon Source, ANL, Argonne, IL 60439, USA

Abstract

A new S-band Photo-Cathode (PC) gun is recently commissioned at the Advanced Photo Source (APS), Argonne. In this paper we report the high-power RF conditioning process of the gun. Dark current is monitored during the RF conditioning. Following the RF conditioning, photo-electron beams are generated from the gun. The quantum efficiency of the copper cathode is monitored. Normalized beam emittance at different drive-laser sizes is measured as a function of solenoid strength, RF gradient and phase. Beam energy is also measured in a spectrometer.

THE APS PC GUN

The APS PC gun is a LCLS type gun [1-3] fabricated by SLAC. The gun is delivered to APS Oct. 2013 and installed at the Injector Test Stand (ITS) Dec. 2013.

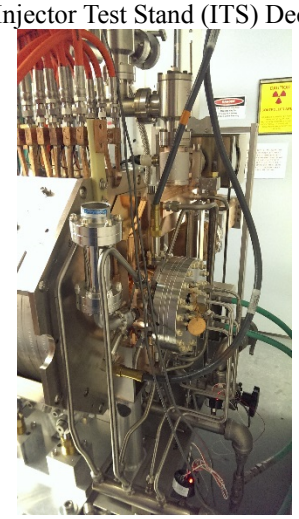

Figure 1: The S-band photo-cathode RF gun and solenoid as installed at the ITS.

HIGH POWER RF CONDITIONING

High power RF conditioning of the PC gun started on March 5, 2014. Forward RF power of 12 MW, pulse length 2.5 μs and 30 Hz repetition rate were successfully achieved on March 20, 2014.

To protect the gun from damaging during RF conditioning, three types of interlocks are implemented: reflected RF power, vacuum pressure and arc detector installed on the view port of the cathode cell.

The waveforms of the forward and reflected RF at the gun waveguide are saved at different RF power levels. An example is shown in Figure 2. Furthermore, waveforms of the field probes of the half-cell and full-cell are also collected, see Figure 3.

*Work supported by U.S. Department of Energy, Office of Science, under Contract No. DE-AC02-06CH11357.
#yinesun@aps.anl.gov

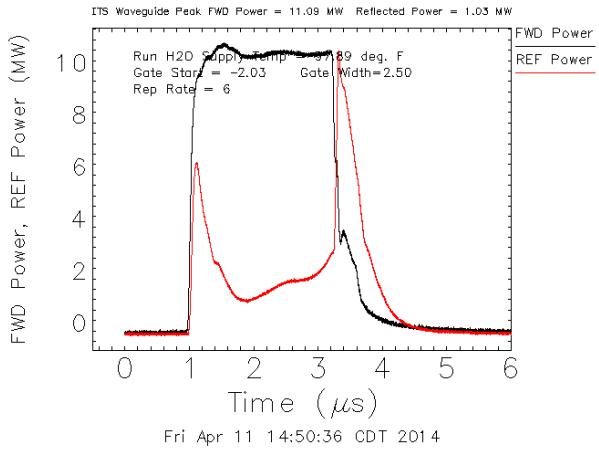

Figure 2: The forward and reflected RF waveforms at the gun waveguide.

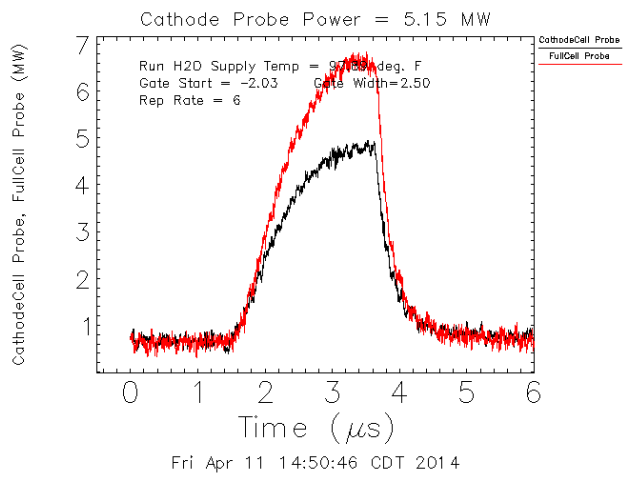

Figure 3: The cathode half-cell and the full cell field probe waveforms.

Dark currents are measured using the ICT at different solenoid strengths and RF power levels. A set of ICT measurements at 12 MW forward RF power, solenoid current ranging [20 ~ 240] A are plotted in Figure 4.

The total charge is calculated from integrating the current monitor waveforms. At different RF repetition rate, the dark current collected by the ICT varies as the solenoid current is changed, see Figure 5. The maximum dark current per RF pulse observed during the RF conditioning is less than 150 pC.

ISBN 978-3-95450-133-5

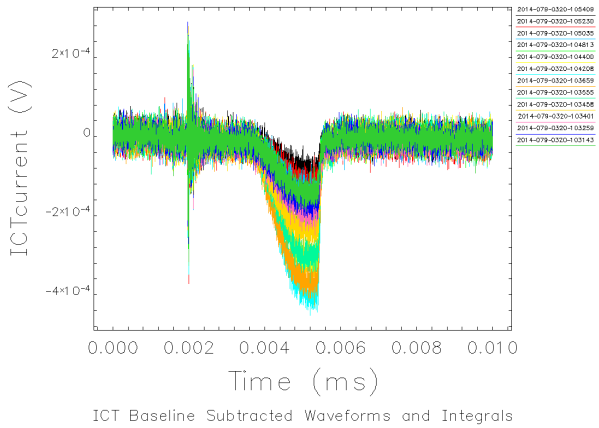

Figure 4: ICT waveforms as solenoid current is varied from 20A to 240A in 20A steps.

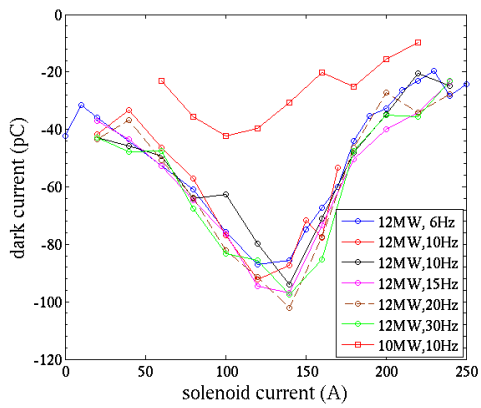

Figure 5: Dark current measured during RF conditioning of the PC gun.

ELECTRON BEAM COMMISSIONING

Following the successful high power RF conditioning, photo-electron beam commissioning of the PC gun in ITS started on April 10, 2014.

The ITS Beamline

The ITS beamline starts with the photocathode RF gun, followed by its main solenoid embedded with its quadrupole and dipole corrector magnets [4]. The major components of the beamline elements are illustrated in Figure 6. Three quadrupoles and three horizontal/vertical steering magnets, an integrated current monitor (ICT), a YAG screen and a Faraday cup are available in the straight-ahead beamline. The transverse emittance is measured by scanning one or two of the three quadruple strengths and measure the beam size on the straight line YAG screen. Photo-electron bunch charge as well as dark current are measured by the calibrated ICT. The Faraday cup signal is used to maximize the beam transmission to the end of the beamline.

A spectrometer dipole magnet bends the beam by 45° and forms the bend line for beam energy and energy spread measurements. The bend line consists of two quadrupoles, a YAG screen and a Faraday cup.

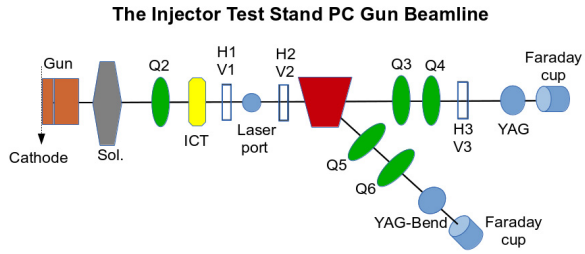

Figure 6: Layout of the Injector Test Stand photo-cathode RF gun beamline.

Cathode Quantum Efficiency

On the optical table inside the ITS, the drive-laser goes through a splitter, 85% of the laser is transported to photo-cathode and the rest is used for laser beam diagnostics including transverse profile monitoring on a virtual cathode, and laser energy measurement on a calibrated energy meter (EM3); see Figure 7.

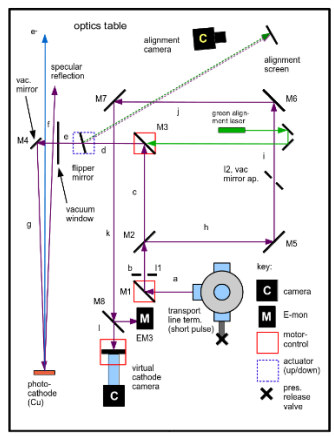

Figure 7: PC gun drive laser path on the optical table inside the ITS room.

As the gun RF phase is scanned, the photo-electron charge emitted is recorded to form a phase scan curve. Varying RF power s from 1 ~ 11 MW, the phase scan curves in Figure 8 are obtained. We see from Figure 8 that at RF power above 4.9 MW, the Schottky enhancement of the quantum efficiency is very pronounced.

The quantum efficiency (QE) is the number of emitted electrons per photon. In practical units for 263 nm drive-laser wavelength, the QE of cathode can be calculated via Eq. (1),

$$QE = \frac{Q(pC)}{U(\mu J)} x 4.7 x 10^{-6}, \quad (1)$$

where Q is the bunch charge in pC, U is the UV energy on cathode. For example, for 10 μJ UV laser, 21 pC bunch charge, the QE is $1x10^{-5}$. The measured QE as a function of the accelerating gradient is shown in Figure 9.

ISBN 978-3-95450-133-5

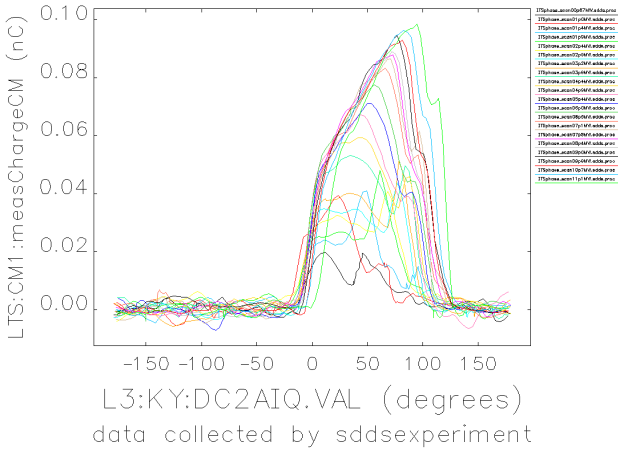

Figure 8: RF phase scan of the gun. Horizontal axis is the RF phase of the gun klystron, and vertical is the bunch charge measured by the ICT.

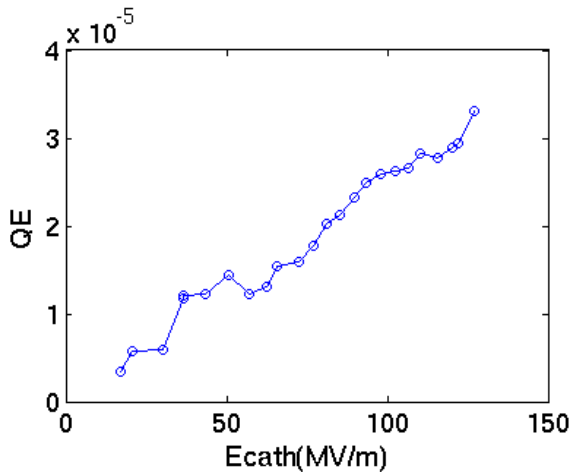

Figure 9: Quantum efficiency at different accelerating gradients on the cathode, UV laser energy at 16 µJ.

A quantum efficiency mapping of the cathode in a 2.5 mm by 2.5 mm square area was performed. The drive-laser position is controlled by a stepping motor and its location on the virtual cathode is recorded. The QE ranges from 3.2×10^{-5} to 3.8×10^{-5}, see Figure 10.

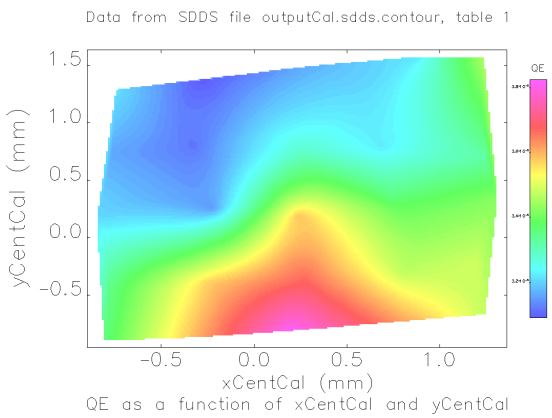

Figure 10: Quantum efficiency mapping of the cathode.

Transverse Emittance

The transverse emittance is measured using a quadrupole scan technique. The strengths of one or two quadrupoles in the straight beamline are varied while transverse beam size is measured on the YAG screen. The YAG screen is a 100 µm thick YAG crystal with a 0.5" diameter holder.

Emittances are measured for different bunch charges and drive-laser spot sizes, as the gun accelerating gradient, phase and solenoid current are varied systematically. The laser spot size is controlled by inserting a pinhole in the laser path. Images of the drive-laser on the virtual cathode are shown in Figure 11.

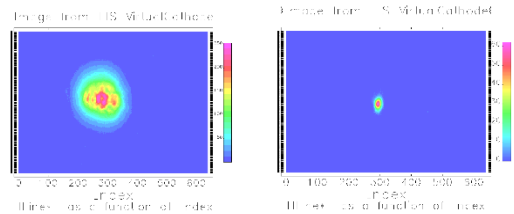

Figure 11: Virtual cathode images of the photo-cathode drive-laser. In the left image, the rms spot size is ~ 0.6mm; on the right image, a 0.8 mm pin hole and a focusing telescope are used to create an rms sport size of 92 µm by 179 µm. The cause for the asymmetry in the right image is under investigation.

The best emittance obtained for bunch charge ~25 pC is ~0.8 µm; see Figure 12 for measured emittances at different RF power and phase as the solenoid current is varied.

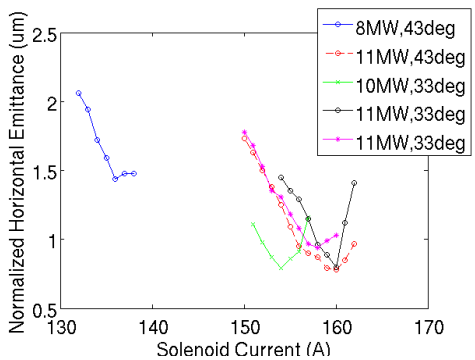

Figure 12: Normalized emittance measured for bunch charge ~ 25 pC.

To get higher bunch charge, the 0.8 mm pin hold was replaced by a 1.0 mm pin pole. An UV attenuator is used to control the drive-laser intensity to further control the bunch charge. At a bunch charge of ~ 100 pC, the smallest normalized emittance measured is ~2.1 µm with 0.6 mm rms drive laser size; see Figure 13.

ISBN 978-3-95450-133-5

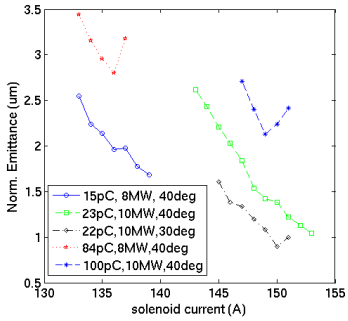

Figure 13: Normalized emittance measured with the 1 mm diameter pin hole inserted in the drive laser path.

Energy and Energy Spread

Beam energy is measured using a 45º sector spectrometer dipole magnet. Beam-based alignment if performed to ensure that the beam goes through the electrical and magnetic center of the PC gun, solenoid and the quadrupole upstream of the spectrometer dipole. At proper current of the spectrometer dipole, the beam goes through the center of the quadrupoles downstream of the dipole in the bend line, and beam centroid location on the bend line YAG is recorded.

As we change the gun gradient and phase, the beam energy is can be obtained from the magnetic field given the excitation current of the spectrometer dipole. Beam energy > 6 MeV is achieved. An example of measured beam energy at different RF phase and 10MW forward power is shown in Figure 14; corresponding energy spread is shown in Figure 15.

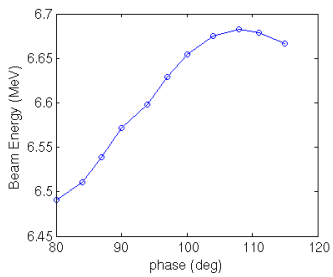

Figure 14: Measured beam energy at 10 MW forward power as the gun rf phase is varied

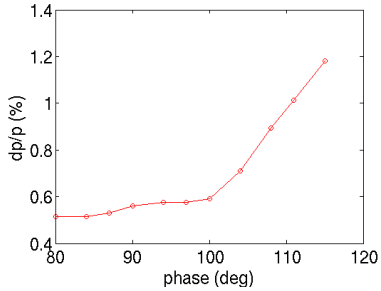

Figure 15: Measured relative energy spread for a ~35 pC bunch charge at 10 MW forward power as the gun rf phase is varied.

ACKNOWLEDGMENT

We wish to thank Norbet Holtkamp, Erik Jongewaard, Feng Zhou, Juwen Wang and Jim Lewandowski from SLAC for providing helpful information related to the PC gun. The many useful discussions with John Power from the AWA group of Argonne, Nicholas Sereno and Michael Borland at APS, Alex Lumpkin of Fermilab, are greatly appreciated. The installation and commissioning of the PC gun at ITS would not be possible without the support from the mechanical, survey and alignment, vacuum, water, electrical power, diagnostics and controls group.

REFERENCES

[1] C. Limborg et al., "RF Design of the LCLS Gun," LCLS-TN-05-3, Feb. 2005.

[2] D. H. Dowell et al., "Results of the SLAC LCLS Gun High-Power RF Tests," WEPMS036, PAC'07, Albuquerque, New Mexico (2007).

[3] D. H, Dowell et al., "Commissioning Results of the LCLS Injector," WEAAU0, FEL'07, Novosibirsk, Russia (2007).

[4] J. Schmerge, "LCLS Gun Solenoid Design Considerations," LCLS-TN-05-14, June 2005.

ISBN 978-3-95450-133-5